Published in final edited form as:
Langmuir. 2010 November 16; 26(22): 17703–17711. doi:10.1021/la101960v.

Ferromagnetic Micropallets for Magnetic Capture of Single Adherent Cells

Nicholas M. Gunn[1], **Ruth Chang**[2], **Trisha Westerhof**[3], **Guann-Pyng Li**[4,5,6], **Mark Bachman**[4,5,6], and **Edward L. Nelson**[7,8,9,*]

[1] School of Engineering, Department of Biomedical Engineering, University of California at Irvine, Irvine, CA 92697

[2] Department of Medicine, University of California at Irvine, Irvine, CA 92697

[3] School of Biological Sciences, University of California at Irvine, Irvine, CA 92697

[4] Department of Electrical and Computer Science, University of California at Irvine, Irvine, CA 92697

[5] Integrated Nanosystems Research Facility, University of California at Irvine, Irvine, CA 92697

[6] California Institute for Telecommunications and Information Technology (CalIT^2), University of California at Irvine, Irvine, CA 92697

[7] School of Medicine, Department of Medicine, Division of Hematology/Oncology, University of California at Irvine, Irvine, CA 92697

[8] Institute for Immunology, University of California at Irvine, Irvine, CA 92697

[9] School of Biological Sciences, Department of Molecular Biology and Biochemistry, University of California at Irvine, Irvine, CA 92697

Abstract

We present a magnetic micropallet array and demonstration of its capacity to recover specific, individual adherent cells from large populations and deliver them for downstream single cell analysis. A ferromagnetic photopolymer was formulated, characterized, and used to fabricate magnetic micropallets, which are microscale pedestals that provide demarcated cell growth surfaces, with preservation of biophysical properties including photopatternability, biocompatibility, and optical clarity. Each micropallet holds a single adherent cell in culture and hundreds of thousands of micropallets compose a single micropallet array. Any micropallet in the array can be recovered on demand, carrying the adhered cell with it. We used this platform to selectively recover single cells, which were subsequently analyzed using single cell RT-qPCR.

1. Introduction

Understanding the biology of individual cells within complex microenvironments has proven to be a particular challenge despite the increasing number and variety of tools available for analysis of single cells at the cellular and molecular levels, including microscopy, polymerase chain reaction (PCR), patch-clamp, and microanalytical chemical separations[1–6]. One obstacle to being able to gain this understanding is the limited set of

enelson@uci.edu.

Supporting Information Available: Movie S1 shows magnetic micropallets made from 1:50 FM1002F being attracted by a permanent magnet. This information is available free of charge via the Internet at http://pubs.acs.org/.

tools that permit the selection of a single cell of defined phenotype from a large cellular population, e.g., fluorescence-activated cell sorting (FACS) or laser capture microdissection[1,7,8]. The repertoire of available tools is further diminished when one is interested in recovering a single *adherent cell* from culture with minimal cellular perturbation, i.e., without the need to strip the cell from the growth surface such as is required with popular cell sorting technologies such as FACS or if maintenance of cellular viability is important.

Our group has previously reported the development of a novel microtechnology for the isolation and collection of single adherent cells from large heterogeneous populations[9–12]. This "micropallet array" technology is a unique cell-handling platform that comprises hundreds of thousands of microscale pedestals ("micropallets"). Micropallet arrays are constructed using standard photolithographic techniques from high aspect photoresist and the technology was developed using the popular epoxy-based negative photoresist SU-8. Recently we have developed a new high aspect negative photoresist, called "1002F photoresist", for micropallet array fabrication[13]. 1002F photoresist is similar to SU-8, but offers improved biophysical properties over SU-8, specifically markedly lower autofluorescence across a broad range of UV and visible light wavelengths and increased biocompatibility and support for cell adhesion as compared to SU-8[13].

Each micropallet of the array can hold a single cell in culture and any one micropallet can be selectively released from the substrate using a focused laser pulse, Figure 1A[10–12]. Viability of the adherent cell is maintained throughout the release process and subsequent recovery[11,12]. Released micropallets come to rest on the surface of the array, Figure 1B, and were originally collected via a simple inversion process that allows them to fall freely into an array of collection wells, Figure 1C[11,12]. This process requires that the micropallet array be temporarily sealed against an array of collection wells and the whole configuration inverted 180 degrees. Gravity causes any micropallets not attached to the substrate (i.e., released micropallets) to fall onto the array of collection wells and settle into one or more wells. Any liquid that was covering the micropallet array at the beginning of the transfer process is also transferred such that it now is covering the collection wells. Although this process provided proof of principle for recovery of single adherent cells from the micropallet array, it has many obvious drawbacks. These include: the inadvertent collection of non-target cells that lose adherence to micropallets, the transient exposure to air for the remaining adherent cells on the micropallet array, the large volume of collection fluid, the requirement to search the array of collection wells to locate collected micropallet(s), and very low through-put capacity. Nevertheless, this collection strategy may be appropriate for clonal expansion of limited numbers of collected cells. However, for single cell molecular analyses such as DNA or RNA based PCR analysis or similar single cell investigations, a much smaller collection volume is required and higher throughput is desired. Thus, refinements are needed to enable the efficient application of the micropallet technology to single cell analyses that will enable biologists to dissect the biology of single cells in complex cell mixtures and tissues.

We have recently developed a new strategy to collect and transfer micropallets after release from the micropallet array. The cornerstone of this strategy is to endow the micropallets with susceptibility to magnetic fields, which is accomplished by incorporating magnetic material, namely ferromagnetic nanoparticles, into their structure. The resultant ferromagnetic micropallet could have a level of ferromagnetic responsiveness sufficient to allow its manipulation using low-strength magnetic fields, potentially enabling capture of individual micropallets using small permanent or electro- magnets and transfer to analysis vessels with limited fluid volumes, Figure 1D. The properties of the micropallets that make micropallet arrays especially effective in sorting adherent cells, i.e., their biocompatibility,

ability to be coated with extracellular matrix protein coatings, transparency at the wavelengths of visible and UV light, and low autofluorescence, should not be compromised if this refinement to the micropallet array technology is to be broadly applicable to biological studies. This paper presents our work to realize a ferromagnetic micropallet with preservation of these critical biophysical properties and development of a micropallet array in which each individual micropallet can be magnetically manipulated after its release from the array.

2. Experimental

Preparation of Ferromagnetic Photoresist

Ferromagnetic photoresist (FM1002F) was prepared by mixing dry iron (II,III) oxide nanoparticles (<50 nm particle size (TEM), ≥98% trace metals basis) (Sigma-Aldrich, St. Louis, MO) into 1002F photoresist. The 1002F photoresist was prepared as previously described[13] by dissolving EPON resin 1002F (phenol, 4,4′-(1-methylethylidene)bis-, polymer with 2,2′-((1-Methylethylidene)bis(cyclohexane-4,1-diyloxymethylene))bisoxirane) (Miller-Stephenson, Sylmar, CA) and UVI-6976 photoinitiator (triarylsulfonium hexafluoroantimonate salts in propylene carbonate, Dow Chemical, Torrance, CA) in γ-butyrolactone (GBL) (Sigma-Aldrich, St. Louis, MO) at a ratio of 61% 1002F resin/6.1% photoinitiator/32.9% solvent (weight percentage).

The iron oxide nanoparticles (FeNPs) were added to 1002F photoresist at seven different doping ratios, measured by weight, to create FM1002F with different levels of FeNP content. The set of doped photoresists ranged from 1:200 to 1:2 doping by weight (nanoparticles:1002F) and consisted of: [1:200, 1:100, 1:50, 1:20, 1:10, 1:5, 1:2]. The dry nanoparticles were mixed into 1002F photoresist via mechanical stirring using a RW 20 digital mechanical stirrer (IKA, Wilmington, NC) at 300 RPM for 30 min to create a suspension of nanoparticles in 1002F photoresist. The suspension was centrifuged at 2600 × g for 30 min to pellet aggregates of nanoparticles and the supernatant was collected as the final preparation of FM1002F. The FM1002F was used within 48 h to avoid further settling of nanoparticles, even though noticeable settling was not observed for up to one week after preparation.

X-ray Microanalysis

To quantify the amount of ferromagnetic material present in fabricated structures (e.g., micropallets), samples of FM1002F were analyzed using energy dispersive X-ray spectroscopy to determine elemental iron content. The samples were spin-coated on glass slides, flood exposed with UV radiation and hard-baked, which is analogous to the processing of FM1002F during the fabrication of microstructures. Samples of all doping ratios were prepared along with a duplicate set prepared identically, except that the ferromagnetic photoresist was not centrifuged during preparation. Analysis was performed using a Zeiss EVO LS15 scanning electron microscope equipped with a Thermo System 7 energy dispersive X-ray microanalysis system to obtain measurements at five points across the slide for each sample, which were averaged. A unitless ratio of iron content to carbon content was found for each sample, which was then used to back-calculate the content of FeNPs in the fabricated structures, as described in the Results and Discussion section.

Spectral Analysis of FM1002F Transparency

The seven preparations of resist described above, along with standard 1002F, were spin-coated, flood exposed with UV radiation and hardbaked to create uniform, solid, 50 μm thick coatings on standard 1 × 3 in glass slides. The transmission spectra of the samples were determined using an USB2000 spectrometer (Ocean Optics, Dunedin, FL) to measure

the transmittance of light from a DT 1000 CE UV/Vis light source (Analytical Instrument Systems, Flemington, NJ). Samples were analyzed such that the light was incident on the photoresist-coated side of the slide and transmission was detected at the reverse side. For each sample, the transmissions at five points across the slide were measured and averaged to formulate each data point.

Study of Cell Viability on FM1002F

Biocompatibility of the FM1002F was investigated using solid substrates prepared in the same manner as described above. Substrates of 1002F at doping ratios of 1:20 and 1:10 were prepared, as well as undoped 1002F and plain glass slides for comparison. Plastic 4-well chambers taken from LabTek chamber slides (Nunc, Inc., Naperville, IL) were reattached to the photoresist substrates using polydimethylsiloxane (PDMS) to demarcate 9 × 20 mm regions for each experiment. The substrates were coated with human plasma fibronectin (Millipore, Billerica, MA) to provide an extracellular matrix (ECM) protein coating for cellular attachment, as previously described[14]. Briefly, fibronectin, diluted to 20 μg/ml in phosphate buffered saline (PBS), was applied to each chamber, incubated at room temperature for 1 hr and washed with PBS. NIH/3T3 fibroblast cells (CRL-1658, ATCC, Manassas, VA) were applied to the photoresist substrates at seeding densities of 5,000 cells/ml/well and incubated at 37 °C and 10% CO_2 to permit cellular proliferation. A total of eight wells were initially seeded for each substrate, to be analyzed at various time points, specifically 24 h, 48 h, 72 h and 96 h. Two wells were analyzed per time point. The cells were collected using trypsin-EDTA solution (0.25% trypsin; 1mM EDTA) and the number of cells recovered per well was determined using an Accuri C6 flow cytometer (Accuri Cytometers, Inc., Ann Arbor, MI) with identical gating (encompassing only healthy cells) for each sample.

Photolithographic Patterning of FM1002F

To assess the impact of incorporation of FeNPs into 1002F photoresist on its capacity to construct microstructures, the set of FM1002F photoresists were patterned into microstructures. Photolithographic patterning was performed according to the recipe for plain 1002F photoresist, which uses standard lithographic techniques and was previously described[13,14]. Briefly, 50 μm thick coatings of FM1002F photoresist were obtained by spin-coating and baking the photoresist on clean 1 × 3 in glass slides. The microstructures were patterned by exposure to collimated UV light (6 mW/cm^2) (Oriel, Newport Stratford, Inc., Stratford, CT) through a photomask for 200 s (total energy of 1200 mJ/cm^2) and post-exposure baked, developed with SU-8 developer (MicroChem, Newton, MA), and hardbaked at 120 °C. For doping ratios 1:5 and 1:2, the length of UV exposure was increased to 260 s (total energy of 1560 mJ/cm^2) to compensate for attenuation of the UV light by the nanoparticles. The aim of the photomask's pattern was to test the achievable limits (minimal critical dimension and aspect ratio) for the FM1002F photoresists; it consisted of a dark-field pattern of arrayed squares with variable sizes (25 μm to 200 μm side length) and spacings (10 μm to 75 μm).

Fabrication of Magnetic Micropallet Arrays

FM1002F photoresists at doping ratios of 1:200 to 1:10 were used to fabricate micropallet arrays with the following dimensions: each micropallet had a 40 × 40 μm cross section, 50 μm height, and 30 μm spacing between neighboring micropallets. Microfabrication was completed using the previously-described protocol[13,14] for fabricating micropallet arrays with standard 1002F photoresist, and is the same protocol used to investigate the photopatternability of FM1002F, described above. As described previously[9,14], the micropallet arrays were treated with silane vapor deposition using (heptadecafluoro-1,1,2,2-tetrahydrodecyl)trichlorosilane (Gelest, Morrisville, PA) to create a highly hydrophobic

silane monolayer on the micropallet and glass surfaces. This hydrophobicity causes air to become trapped in the inter-micropallet spaces upon wetting of the arrays and these “air walls” or “virtual walls” serve as the mechanism for cell sequestration to the top surfaces of individual micropallets[9,14]. We observed that the incorporation of iron nanoparticles into the 1002F photoresist did not impact the effectiveness of the silane treatment to support virtual walls. To complete fabrication, LabTek chamber slides were attached to the micropallet arrays using PDMS as described above[14] and held cell culture media and other reagents for subsequent experiments.

Coating of Magnetic Micropallets with Biomolecules

To support cellular adhesion, particularly for primary cells, micropallets must be coated with an appropriate biomolecule or ECM coating. We have previously reported methods to effectively coat micropallet arrays with a variety of ECM coatings, including fibronectin, collagen, and laminin, such that each individual micropallet has a uniform and well-adhered coating on its top surface[14]. The adhesion and uniformity of fibronectin coatings on micropallet arrays fabricated from 1:50 and 1:10 preparations of FM1002F were investigated and compared to fibronectin coatings on micropallet arrays made from standard 1002F.

Fibronectin was applied to the ferromagnetic micropallets as described above and previously reported[14]. For characterization of coating efficiency using fluorescent imaging, fibronectin was detected by immunofluorescence using anti-fibronectin rabbit polyclonal antibody (Cat # F3648, Sigma-Aldrich, St. Louis, MO) as the primary antibody and FITC-conjugated AffiniPure F(ab′)2 fragment donkey anti-rabbit IgG (H+L) as the secondary antibody (Cat # 711-096-152, Jackson ImmunoResearch, West Grove, PA). The antibodies were used according to the manufacturers’ instructions. Negative controls to measure nonspecific binding of the antibodies included 1) arrays not coated with fibronectin and subjected to the full staining protocol and 2) omission of the primary anti-fibronectin antibody. Imaging was done using an LSM 510 Meta laser scanning confocal microscope with appropriate FITC filter set.

Immunofluorescent Imaging of Cells on Magnetic Micropallets

Rat neu-expressing NIH/3T3 cells (CRL-1915, ATCC, Manassas, VA) were plated onto fibronectin-coated micropallet arrays made from FM1002F doped at 1:50 and 1:10 ratios. After an incubation period of 3 h at 37 °C/10% CO_2 to allow for cellular adherence, the cells were stained with antibodies against rat neu and the Hoechst 33342 nuclear stain as follows. The micropallet array was washed x2 with Blocking Buffer (Hanks Buffered Saline Solution (HBSS) with 6% Bovine Serum Albumin (BSA) and 0.1% sodium azide), followed by incubation in Blocking Buffer for 30 min. The array was washed x2 with Staining Buffer (HBSS with 1% BSA and 0.1% sodium azide), followed by 30 min incubation with 0.5ug/ml rat neu monoclonal antibody (clone 7.16.4, EMD/Calbiochem, San Diego, CA) in Staining Buffer supplemented with 20ug/ml Hoechst 33342 (Invitrogen, Carlsbad, CA). The array was washed x5 with Staining Buffer, incubated for 30 min with 4ug/ml goat anti-mouse secondary antibody conjugated to Alexa Fluor 488 (Invitrogen), and finally washed x5 with Staining Buffer to remove unbound secondary antibody. All incubations were at 37°C and 10% CO_2 and all buffers were pre-warmed to 37°C.

Release and Collection of Magnetic Micropallets

Individual magnetic micropallets with single adhered cells were released from the glass substrate of the array using a high-powered pulsed laser similar to previously described methods[11,12,15,16]. Briefly, the pulsed laser is focused at the interface of the micropallet and underlying glass substrate and when activated creates a localized plasma within the focal

volume of the laser. A shock wave is produced and the plasma formation results in ablation of the polymer micropallet material within the focal volume. Rapidly expanding gas from the ablative process is trapped between the micropallet and glass substrate and disrupts the polymer-glass interface, dislodging the micropallet from the glass[15,16]. The micropallet is projected into the fluid and comes to rest on the surface of the array, generally within a few millimeters of its initial position. A magnetic probe, consisting of a small, disk-shaped neodymium rare earth magnet, 1 mm in diameter and 0.5 mm in thickness, was then used to collect the micropallet. The magnet was held at the end of a thin, ~0.5 mm in diameter, stainless steel rod, from which it could be removed after collection of a micropallet. During collection the rare earth magnet is simply brought into proximity of the released micropallet. At sufficiently close distance, the force of gravity is overcome by the magnetic force and the micropallet moves into contact with the magnet. The cell that is held on the micropallet can then be delivered to a downstream vessel, e.g., a PCR tube, by delivery of the combined magnet/micropallet/cell assembly.

Single Cell PCR

Magnetic micropallets were used to isolate and recover cells for single cell reverse transcription quantitative PCR (RT-qPCR) analysis as a demonstration of the utility of magnetic micropallets. Rat neu-expressing NIH/3T3 cells were plated on a micropallet array made from 1:50 FM1002F, which was cleaned with RNaseZap (Ambion, Austin, TX) and 70% ethanol before being coated with fibronectin, as above. Cells were allowed to adhere during a 3 h incubation at 37 °C/10% CO_2, and then micropallets holding single cells were released and magnetically recovered as described above. Recovered single cells were lysed for total RNA content, reverse transcribed for cDNA, cDNA preamplified, and analyzed for specific gene expressions by quantitative polymerase chain reaction (qPCR), all using the TaqMan PreAmp Cells-to-Ct Kit (Applied Biosystems, Foster City, CA) according to manufacturer's instructions. Briefly, single magnetic micropallets with adhered single cells were transferred into PCR tubes containing 1 μl cold 1x PBS and 10 μl Lysis Solution with DNase I at 1:100 dilution for cell lysis to release total RNA. Empty micropallets were also collected and processed identically for no template controls (NTC). For reverse transcription (RT) processing, 25 μl RT Buffer, 2.5 μl RT Enzyme Mix, and 12.5 μl Nuclease-free Water was added directly to the PCR tube. For –RT controls, the RT Enzyme Mix was replaced with water. Subsequently, 12.5 μl of cDNA containing reaction was pre-amplified prior to qPCR analysis for mouse β-Actin and rat neu by TaqMan Gene Expression Assays (Mm01205647_g1 for mouse β-Actin and Rn0056651_m1 for rat neu, Applied Biosystems).

3. Results and Discussion

Iron Oxide Nanoparticle Content of Ferromagnetic Photoresist

While the dry iron oxide nanoparticles were readily dispersed in the liquid 1002F photoresist by simple mechanical stirring, a homogeneous monodispersed mixture was not achieved. Rather, aggregates of nanoparticles remained throughout the composite preparation of ferromagnetic photoresist. It was observed that the aggregates were present in the nanoparticles as obtained from the supplier and not a consequence of being mixed with the photoresist. Several attempts were made to disrupt the aggregates, for example by means of more vigorous mechanical stirring, sonication, grinding, etc., however these approaches were not successful. Therefore, centrifugation was ultimately used to greatly improve the homogeneity of the composite ferromagnetic photoresist by pelleting the larger aggregates out of suspension, leaving only single nanoparticles and very small aggregates in suspension.

As described above, the composite FM1002F photoresists were made by mixing FeNPs into 1002F photoresist at seven different weight ratios. However, while useful for nomenclature, these weight ratios are not indicative of the final amount of FeNPs present in structures fabricated from FM1002F. This is due to the loss of a portion of the FeNPs during centrifugation and also the evaporation of solvent from the photoresist during device fabrication, both of which act to alter the weight percentage of FeNPs in the processed FM1002F. During the X-ray microanalysis used to analyze the processed FM1002F samples, electron-excited characteristic x-rays are analyzed to determine elemental makeup of the sample[17]. According to computer simulation based on material properties, the majority of X-rays detected for this analysis were generated from an excitation volume extending from a depth of one micron to six microns into the 1002F material. Thus, the analysis can be considered of the bulk material. Figure 2A shows SEM micrographs and two dimensional maps of elemental iron distribution for 150 μm square areas of samples of 1:10 FM1002F acquired using the Thermo System 7 microanalysis system. Samples of 1:10 FM1002F prepared using centrifugation to remove aggregates, as described above, were compared to samples that were not centrifuged to determine the effects of centrifugation. It is clearly evident that centrifugation of the resist prior to processing resulted in a more homogeneous distribution of FeNPs. However, this had the trade off of greatly reducing, in some cases by more than half, the content of FeNPs in the composite FM1002F photoresists. Figure 2B is a plot showing the FeNP weight fractions of fully processed FM1002F with and without centrifuging for each doping ratio. These were calculated by correcting the prescribed weight ratios (1:200–1:2) to account for evaporation of solvent and then correlating these values with the elemental iron content of non-centrifuged samples as determined by x-ray microanalysis. From this, the FeNP content of the centrifuged samples was calculated.

Light Transmission of Ferromagnetic Photoresist

Variation in bulk light transmission across each sample was very low, which can be attributed to the homogeneity conferred by centrifuge treatment. The largest deviation in transmission (from the mean) for any wavelength for all samples was 6%, and the majority of samples had deviations under 1%. It is important to understand the effect of iron oxide doping of the photoresist on its light transmission for two reasons. The first is so that UV exposure times can be properly adjusted during UV photopolymerization of the photoresist to compensate for increased attenuation of the UV energy by the nanoparticles. The second is for uses of the FM1002F dependent upon the transmissive optical properties of the resist, such as fluorescent imaging of adherent cells as we are reporting. For inverted fluorescent microscopy systems especially, e.g., the laser scanning confocal microscope used in this work where both the excitation and emission light paths pass through the photoresist, attenuation of the light energy must be considered.

Figure 3A shows light transmission versus wavelength for glass, standard 1002F, and each of the FeNP-doped samples. As expected, there is a trend of decreasing transmission with increasing FeNP content, for all wavelengths measured. Attenuation is minimal for low doping ratios, but becomes significant at higher ratios. Attenuation decreases slightly as wavelength increases, which is possibly explained by decreased Rayleigh scattering by the nanoparticles at longer wavelengths. Figure 3B illustrates the attenuation of light versus doping for four specific wavelengths: 365, 405, 495, and 519 nm. These wavelengths were chosen to coincide with the I-lines and H-lines (365 and 405 nm) produced by mercury-based UV exposure systems and the excitation and emission wavelengths (495 and 519 nm) for the popular fluorescent marker, Alexa Flour 488. This figure suggests processing results could be improved by use of a longpass filter to block shorter UV wavelengths and deliver a more uniform UV dosage throughout the thickness of the photoresist. It also indicates that

light energy reaching, as well as being emitted from, fluorophores in immunofluorescent applications will experience greater attenuation with increasing levels of FeNP doping. This may be significant in applications where very weak fluorescent signals are expected.

Biocompatibility of Ferromagnetic Photoresist

The rate of proliferation of 3T3 cells on substrates of FM1002F was used as a metric to measure their biocompatibility. The biophysical properties of the 1002F photoresist has been previously shown to be better than SU-8[13], which itself is frequently used in biological microelectromechanical systems (BioMEMS) devices that are integrated with cells in culture[18–21] and classified as a non-irritant[22]. We compared growth rates on fibronectin-coated substrates of glass, undoped 1002F, and FM1002F at two doping levels. There was no statistical difference amongst growth rates on the various substrates and no correlation was seen between growth rate and nanoparticle doping level, Figure 4, suggesting that incorporation of the nanoparticles did not affect the biocompatibility of the 1002F photoresist. The experiment was designed to encompass the period of fastest growth of the 3T3 cells, which has been previously shown to be 48 to 72 h after plating[23]. For the micropallet array application discussed in this paper and, we believe, for a majority of other cell-interacting applications for which this material would be of use, cells will not remain in contact with the FM1002F for nearly this long of a time period. Conversely, while not expected to exist, long term post-exposure effects on the cells remain unknown. It was noted that throughout this experiment, as well all subsequent experiments, no difference in the morphology, behavior, appearance, or other metric was seen between cells on substrates of FM1002F as compared to standard 1002F.

Photopatternability of Ferromagnetic Photoresist

All preparations of FM1002F, including the most heavily doped 1:2 preparation, were patternable using standard UV lithography techniques. For low doping ratios, i.e., 1:200, 1:100 and 1:50, microstructures had smooth, near vertical sidewalls and were very similar in appearance to microstructures made from standard 1002F, Figure 5A. Microstructures 50 μm in height with 10 μm features could be created with these doping ratios. However, the quality of the microstructure sidewall deteriorates as the amount of FeNPs in the photoresist is increased, as can be seen in Figure 5B, and resolving 10 μm features becomes difficult for doping ratios 1:20 and 1:10. Nevertheless, structures with dimensions near those of standard micropallets (40 × 40 μm and 30 μm gaps) are easily patternable in 50 μm thick coatings of FM1002F doped at ratios as high as 1:10. Microstructures composed of 1:10 FM1002F and of various dimensions that were made using the test photomask can be seen in Figure 5C. Even the most heavily-doped preparation (1:2) of FM1002F was patternable, as can be seen in Figure 5D. 200 × 200 μm pallets with 75 μm or 50 μm gaps were created with 1:2 FM1002F, although adhesion to the glass substrate was partially compromised.

Adherence of Extracellular Matrix Coatings to Magnetic Micropallets

Immunofluorescent imaging confirmed that the deposition and adherence of fibronectin on micropallets was not detrimentally affected by incorporation of FeNPs. Figure 6A is a control image showing minimal background fluorescence from a standard, uncoated micropallet array that was subjected to the full staining protocol. Figures 6B–D show a standard micropallet array and arrays made from 1:50 and 1:10 FM1002F, respectively, which were coated with fibronectin and subsequently evaluated by immunofluorescence for the integrity of the fibronectin coatings. The fibronectin coatings appear similar across all three arrays, although some heterogeneity in the fluorescent signal, seen as bright areas, is observed for the array made from 1:10 FM1002F. While a centrifuge treatment was employed to remove large aggregates of nanoparticles from the ferromagnetic photoresists, some small aggregates remain and are more prevalent with increasing amounts of FeNPs,

possibly accounting for the apparent slight heterogeneity in the fibronectin coating at higher doping ratios, seen best in Panel D. Overall this experiment suggests that a similar amount of fibronectin was deposited on micropallets made from FM1002F as compared to standard 1002F and that the fibronectin was well-adhered and extended to the boundary of the micropallets in all cases.

Immunofluorescent Imaging of Cells on Magnetic Micropallets

Immunofluorescently-labeled rat neu-expressing 3T3 cells were imaged in two fluorescent channels and phase contrast using an LSM 510 Meta laser scanning confocal microscope. As can be seen in Figure 7A, the FeNP content of the micropallets made with 1:50 FM1002F had nearly zero impact on image quality and the cells are clearly visible in all channels. The phase contrast image and fluorescent signals are bright and undisrupted. However, as the amount of FeNPs in the micropallets in increased, the impact on imaging quality also increases. In Figure 7B, which shows cells on micropallets made from 1:10 FM1002F, it is very difficult to discern the presence of all cells using the phase contrast channel. However, the fluorescent signals from the cell surface markers and nuclear stain remain strong and undistorted, thereby allowing easy identification of cells in these channels. Micropallet arrays imaged in the absence of primary anti-neu antibody revealed no non-specific background staining (data not shown). There is some distortion and attenuation of the fluorescent signals due to aggregates of FeNPs, but it is minimal and overall attenuation of the signal strength is not apparent. Overall, lower doping ratios of FeNPs prove to be more advantageous for imaging purposes and depending on specific applications, e.g., need for cellular identification using the phase contrast channel, a tradeoff of improved imaging quality versus decrease in magnetic attractive force can be made.

Single Cell Recovery Using Magnetic Micropallets

In the case with nonmagnetic micropallets, released micropallets are collected by mating the micropallet array with a separate array of microwells and inverting the whole configuration such that loose micropallets fall into an array of collection wells (please refer to Figure 1). However, magnetic micropallets enable released micropallets to be individually recovered directly from the surface of the array with an appropriate magnetic collection device. A simple collection probe based on a small permanent magnetic was used to easily collect released micropallets. The distance at which the micropallet was captured depended on the amount of FeNPs present in the micropallet. For example, micropallets made from 1:50 FM1002F were captured at a distance of roughly 1–2 mm, whereas micropallets made from 1:10 FM1002F could be captured at a distance of 5 mm or more. See Supporting Information, Movie S1 for a demonstration of the attractability of micropallets made from 1:50 FM1002F. Magnetic micropallets made from all preparations of FM1002F (1:2–1:200) were collectable, although attraction was especially weak at the lower end of the set (1:200).

Micropallets made from 1:50 FM1002F were used for single micropallet/cell collection experiments as this preparation was found to offer the best compromise between optical clarity and magnetic responsiveness. Figures 8A–C show a single micropallet with adhered cell being released from an array and coming to rest on the array’s surface near the point of release. The micropallet is collected directly from this position. Single micropallets can be released and collected without any disturbance of neighboring micropallets or nearby cells. Figure 8D shows the micropallet and single cell after recovery being held by a 1 mm diameter neodymium rare earth magnet. The magnetic force holds the micropallet to the magnet throughout the collection procedure and passage through air-liquid interfaces after capture. Such passages are necessary to transfer the micropallet and cell to downstream vessels, such as tissue culture plates or PCR tubes. Micropallets made from FM1002F at

doping ratios of 1:50 and greater (i.e., 1:20, 1:10) were held firmly to the magnet during this process.

Single Cell PCR Analysis

Since the micropallet arrays platform has the potential to be applied to the study of individual cells at the molecular level, it was of interest to establish the feasibility of analyzing the gene expression of recovered individual cells using single cell RT-qPCR. The expression levels of both β-actin and rat neu genes were detected and quantified with RT-qPCR analysis of cDNA that was reverse transcribed and amplified from RNA of single cells recovered using magnetic micropallets and delivered to PCR tubes using small rare earth magnets as described above. Figure 9 shows the amplification curves of 3 individual sets of cells that were recovered and analyzed. Each set included an individual micropallet with a single rat neu-expressing 3T3 cell. Transcripts for both β-actin and rat neu could be detected for each individual cell and –RT controls were negative for cDNA presence. The average threshold cycle (Ct) values for all single cell samples were 26.80 ± 0.26 for β-actin and 22.99 ± 2.20 for rat neu. There is some variability in the expression of rat neu of the three single cells that were analyzed, but this is not unexpected as the cells were not synchronized nor recently subcloned and some variance in rat neu mRNA levels is anticipated between individual cells. Micropallets without cells (NTCs) did not yield a detectable signal over three separate experiments. These data provide proof of principle for the quantitative detection of specific mRNA sequences from single cells recovered from the micropallet array.

4. Conclusions

We have established the capacity to impart magnetic properties to photoresist polymer while maintaining the fundamental biophysical properties that make the photoresist ideally suited for BioMEMS applications. These biophysical properties of the ferromagnetic photoresist include biocompatibility, photopatternability, capacity to support ECM biomolecule coatings, and minimal degradation of both light transmission and optical clarity relative to standard 1002F photoresist. We have demonstrated that varying the doping ratio allows tuning of optical and magnetic properties to accommodate particular applications. This material would also be useful in a multitude of magnetically-actuated microstructure systems, such as magnetically deformable cantilevers for micro-optical applications, mechanical switches in RF-MEMS applications, and magnetically-actuated valves in microfluidics applications, etc.

We have observed strengthened magnetic properties of FM1002F with increasing doping ratios, at the expense of degradation of photopatternability and biophysical properties. This suggests that optimal doping ratios for individual applications will need to be determined. Similarly, we have demonstrated the advantages of centrifugation of the FM1002F mixture prior to photopatterning. Interestingly, we tried using other forms of magnetic nanoparticles to impart magnetic properties, but these resulted in photoresist with deficient optical properties and other characteristics that compromised the resultant microstructures. In similar work reported by Damean et al.[24], nickel nanospheres were incorporated into SU-8 to create magnetically-actuatable cantilevers, but the maximum doping ratio reported was only 1:6.51 (13.3% nanospheres by weight). Thus, the choice of magnetic compound is also an important consideration that affects magnetic and optical properties and processing capabilities.

The ferromagnetic photoresist described herein was used to refine an advanced cell analysis platform for adherent cells, micropallet arrays, by creating magnetically-manipulatable micropallets. The ability to magnetically collect and manipulate released micropallets

greatly improves system throughput and paves the way for automation of the collection process. In addition to improved throughput, magnetic manipulation enables the transfer of individual released micropallets with remarkably increased precision. Afforded this new capability, we used the magnetic micropallet arrays platform to isolate and perform single cell RT-qPCR analysis on single cells positively selected and recovered from a population of over 10,000 cells. The ability to collect and transfer released micropallets via magnetic means allows rapid, sequential release and recovery events without the problems associated with use of nonmagnetic micropallets. Also, importantly for single cell PCR analysis, the collected micropallet and cell can be delivered directly into PCR analysis reagents, i.e., lysis buffer, in a PCR tube. Such analysis requires transfer of the cell into very small volumes of liquid (~ 10 μl) and thus would not be possible using prior collection methods, i.e., the previously described inversion technique that is required for collection of nonmagnetic micropallets, as this method delivers the micropallet in a very large volume of liquid. Thus, this refinement of the micropallet array overcomes several drawbacks of earlier renditions of the technology, expressly: 1) generally only one micropallet could be released and collected in each inversion process (due to confusion of micropallet identities if multiple, unindexed micropallets were simultaneously released and collected), 2) in the inversion method, the array of collection wells must be scanned to locate released micropallets, and 3) by nature of this method, collected micropallets were present within a relatively very large volume of liquid after collection.

The addition of magnetic properties to the micropallet array provides greatly improved functionality to the base platform while not impeding any of the virtues that makes micropallet arrays a unique and powerful cell handling technology. This opens the opportunity for development of more efficient tools and devices to further improve collection and handling of released individual micropallets. In the future, collection probes based on electromagnets, or which cleverly utilize permanent magnets, can be made such that micropallets are collected and delivered sans magnet. This paper presents the first, foundational step towards the next generation of the micropallet arrays platform and further BioMEMS devices constructed from ferromagnetic photoresist.

Acknowledgments

This work was supported by the following research awards from their respective parent organizations: National Institutes of Health (NIH) CA132039, Department of Defense - Congressionally Mandated Medical Research Program (DOD-CDMRP) for Breast Cancer- Synergistic Idea Award BC074212, National Science Foundation's Integrative Graduate Education and Research Traineeship program (NSF-IGERT) Life Chips Award DGE-0549479, and Beckman Laser Institute and Medical Center's Laser Microbeam and Medical Program (LAMMP), award number P41RR001192, from the National Center For Research Resources. The content is solely the responsibility of the authors and does not necessarily represent the official views of the National Center for Research Resources, the National Institutes of Health, or the Department of Defense. Use of the EVO LS15 was generously made available by Carl Zeiss SMT at UCI's Zeiss Center of Excellence. NMG acknowledges the equal involvement and mentorship of MB and ELN.

References

1. Brehm-Stecher BF, Johnson EA. Microbiol Mol Biol Rev. 2004; 68:538–559. [PubMed: 15353569]
2. van Manen H, Kraan YM, Roos D, Otto C. Proceedings of the National Academy of Sciences of the United States of America. 2005; 102:10159–10164. [PubMed: 16002471]
3. Hahn S, Zhong XY, Troeger C, Burgemeister R, KG. Cellular and Molecular Life Sciences. 2000; 57:96–105. [PubMed: 10949583]
4. Zhao Y, Inayat S, Dikin DA, Singer JH, Ruoff RS, Troy JB. Proceedings of the Institution of Mechanical Engineers, Part N: Journal of Nanoengineering and Nanosystems. 2008; 222:1–11.
5. Lu Y, Takeshita T, Morimoto K. Environ Health Prev Med. 1997; 2:53–58. [PubMed: 21432452]

6. Dovichi, NJ.; Hu, S.; Michels, D.; Mao, D.; Dambrowitz, A. Proteomics for Biological Discovery. Timothy, D.; Veenstra, JRY., editors. 2006. p. 225-245.
7. Nicholas CR, Gaur M, Wang S, Pera RAR, Leavitt AD. Stem Cells Dev. 2007; 16:109–117. [PubMed: 17348809]
8. Espina V, Wulfkuhle JD, Calvert VS, VanMeter A, Zhou W, Coukos G, Geho DH, Petricoin EF, Liotta LA. Nat Protocols. 2006; 1:586–603.
9. Wang Y, Sims CE, Marc P, Bachman M, Li GP, Allbritton NL. Langmuir. 2006; 22:8257–8262. [PubMed: 16952271]
10. To'a Salazar G, Wang Y, Young G, Bachman M, Sims CE, Li GP, Allbritton NL. Analytical Chemistry. 2007; 79:682–687. [PubMed: 17222037]
11. Wang Y, Young G, Bachman M, Sims CE, Li, Allbritton NL. Analytical Chemistry. 2007; 79:2359–2366. [PubMed: 17288466]
12. Wang Y, Young G, Aoto PC, Pai J, Bachman M, Li GP, Sims CE, Allbritton NL. Cytometry Part A. 2007; 71A:866–874.
13. Pai J, Wang Y, Salazar GT, Sims CE, Bachman M, Li GP, Allbritton NL. Analytical Chemistry. 2007; 79:8774–8780. [PubMed: 17949059]
14. Gunn N, Bachman M, Li G, Nelson E. JBMR-A. in press.
15. Quinto-Su PA, To'a Salazar G, Sims CE, Allbritton NL, Venugopalan V. Analytical Chemistry. 2008; 80:4675–4679. [PubMed: 18489124]
16. Salazar GT, Wang Y, Sims CE, Bachman M, Li G, Allbritton NL. J Biomed Opt. 2008; 13:034007–034007. [PubMed: 18601552]
17. Goldstein, J.; Newbury, DE.; Joy, DC.; Echlin, P.; Lyman, CE.; Lifshin, E. Scanning electron microscopy and x-ray microanalysis. Springer; 2003.
18. Rowe L, Almasri M, Lee K, Fogleman N, Brewer GJ, Nam Y, Wheeler BC, Vukasinovic J, Glezer A, Frazier AB. Lab Chip. 2007; 7:475–482. [PubMed: 17389964]
19. Li M, Glawe J, Mills D, McShane M, Gale B. 2000; 66:531–36.
20. Choi, Y.; Choi, S.; Powers, R. Allen, Mark Hilton Head Island. South Caroline, USA: 2000. p. 286-289.
21. Musick K, Khatamia D, Wheeler BC. Lab Chip. 2009; 9:2036. [PubMed: 19568672]
22. Kotzar G, Freas M, Abel P, Fleischman A, Roy S, Zorman C, Moran JM, Melzak J. Biomaterials. 2002; 23:2737–2750. [PubMed: 12059024]
23. Thurston G, Palcic B. Cell Motility and the Cytoskeleton. 1987; 7:361–367. [PubMed: 3607895]
24. Damean N, Parviz BA, Lee JN, Odom T, Whitesides GM. J Micromech Microeng. 2005; 15:29–34.

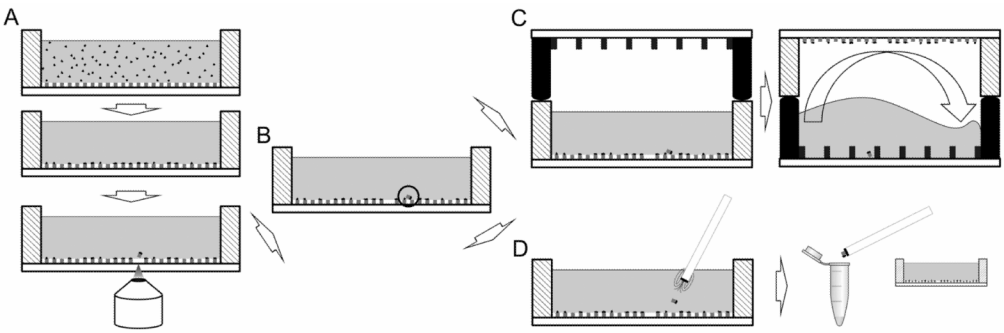

Figure 1. Schematic illustration showing micropallet release and recovery

(A) Method of release of a single micropallet and adhered cell: (Top) Cells are applied to the micropallet array as a suspension of single cells in cell culture media. (Middle) Cells are allowed to settle onto the surface of the array and adhere to individual micropallets over a period of ~3–4 h. (Bottom) Single micropallets can be selectively released using a pulsed laser that is focused at the interface of the micropallet and glass substrate. (B) After release, the micropallet, circled, comes to rest on the surface of the array, from where it remains to be collected. (C) Traditional method of collection of released micropallets: (Left) An array of collection wells with rubber gasket is temporarily mated to the micropallet array by pressing the two together. (Right) The configuration is inverted, which transfers the liquid and any released micropallets onto the array of collection wells. The released micropallet settles into a well at random. (D) The magnetic collection method described in this paper: (Left) The micropallet can be collected with the use of a magnetic probe. When the probe is brought near the micropallet, the micropallet moves into contact with it due to magnetic attraction. (Right) The micropallet and adhered cell can be delivered precisely to any location or downstream analysis vessel, e.g., a PCR tube.

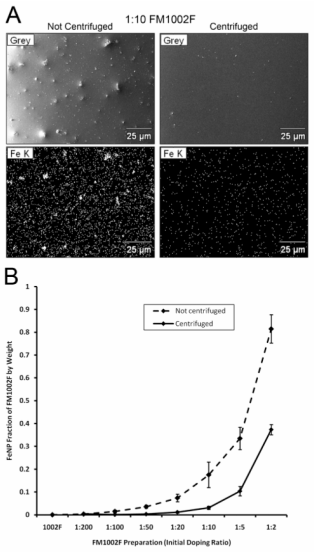

Figure 2. Iron oxide nanoparticle (FeNP) content of the ferromagnetic 1002F photoresist (FM1002F)

Iron content was characterized using X-ray microanalysis. Centrifugal treatment of the liquid FM1002F preparations had the effect of removing aggregates of nanoparticles. (A) Top row: SEM micrographs of samples of 1:10 FM1002F that was prepared without (left) and with (right) centrifugal treatment. Uniformity of the surface was greatly improved with centrifugation. Bottom row: Two dimensional mapping of elemental iron of the same fields of view as Top row. The non-centrifuged sample (left) has more overall iron content, but the centrifuged sample (right) has much improved homogeneity of iron distribution. (B) Graph of FeNP content, by weight fraction, of the various FM1002F preparations with (solid line) or without (dashed line) centrifugal treatment. The FeNP content was dramatically reduced by centrifugation.

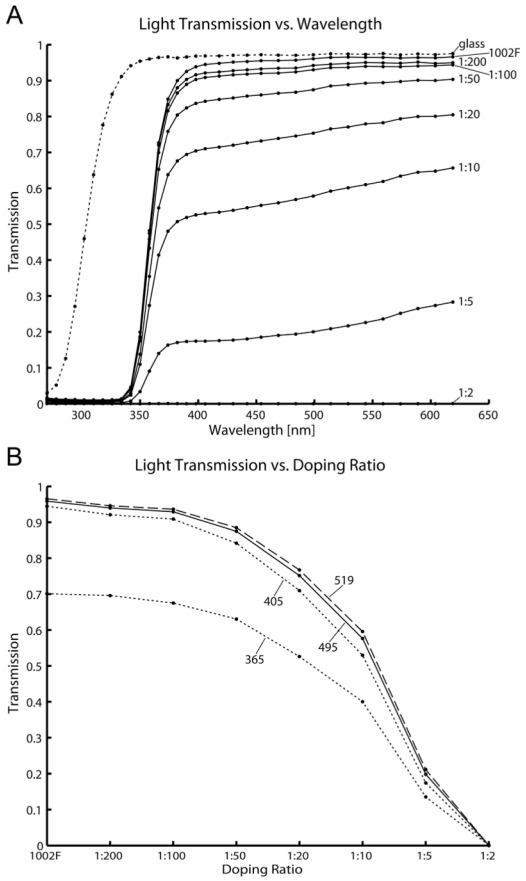

Figure 3. Light transmission of FeNP doped-1002F

The transmission of light through the FM1002F preparations and standard 1002F was measured across a range of wavelengths. (A) Graph of transmission versus wavelength. The transmission for all wavelengths decreased as FeNP content was increased. (B) Graph for transmission versus doping ratio for four specific wavelengths. 365 nm and 405 nm correspond to the H and I lines, respectively, of mercury lamps used for UV exposure during photolithography, and 495 nm and 519 nm are the excitation and emission wavelengths, respectively, for the popular fluorescent marker, Alexa Flour 488.

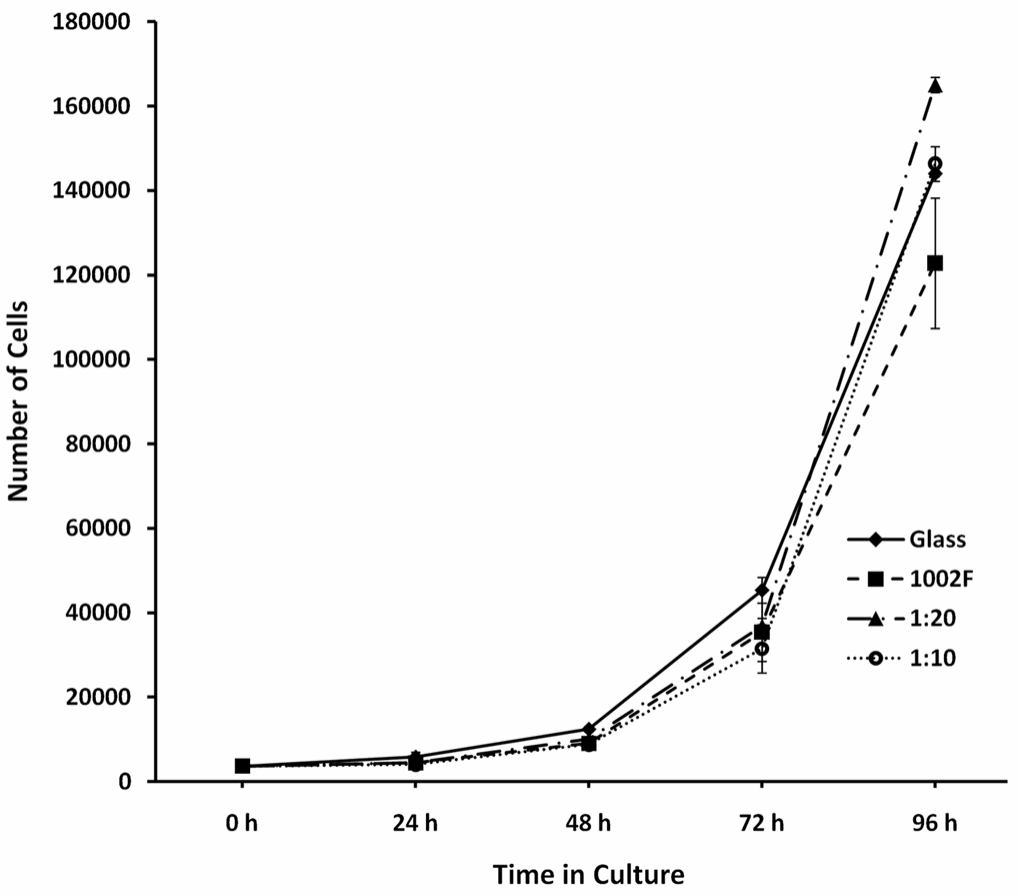

Figure 4. Biocompatibility of FeNP-doped 1002F

Plot showing growth rate of NIH/3T3 cells on fibronectin-coated substrates of glass, 1002F, 1:20 FM1002F and 1:10 FM1002F. There is not a statistical difference between growth rates for cells on the different substrates and there is no correlation between growth rate and level of FeNP doping, suggesting the presence of FeNPs in the substrate did not affect cellular behavior.

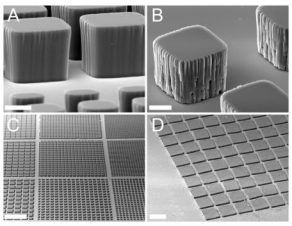

Figure 5. Photopatternability of FeNP-doped 1002F

FM1002F was spin coated to create 50 μm thick layers and photopatterned using a photomask with a test pattern of various dimensions. SEM micrographs were obtained: (A) 50 × 50 μm and 25 × 25 μm (foreground) pallets made from 1:200 FM1002F. Scale bar is 25 μm. (B) 50 × 50 μm pallet made from 1:10 FM1002F. The increased amount of nanoparticles in the FM1002F affects the appearance of the microstructure sidewalls, but the photopatterning of small structures remains practical. (C) Pallets of various dimensions made from 1:10 FM1002F. The test pattern consisted of arrays of squares with side lengths of 25–200 μm and spacings of 10–75 μm. Scale bar is 1 mm. (D) 200 × 200 μm pallets with 50 μm spacings made from 1:2 FM1002F. Scale bar is 250 μm.

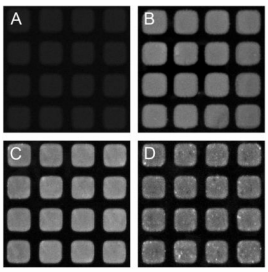

Figure 6. Capacity to support extracellular matrix component coatings

Micropallets made from 1002F or FM1002F were coated with fibronectin that was subsequently immunofluorescently labeled. Immunofluorescent micrographs were obtained using a scanning laser confocal microscope. Micropallets are 40 × 40 μm. (A) Control image for which the full staining protocol was performed on micropallets made from standard 1002F, but not coated with fibronectin. (B, C, and D) Fluorescent images of fibronectin-coated micropallets made from standard 1002F, 1:50 FM1002F, and 1:10 FM1002F, respectively.

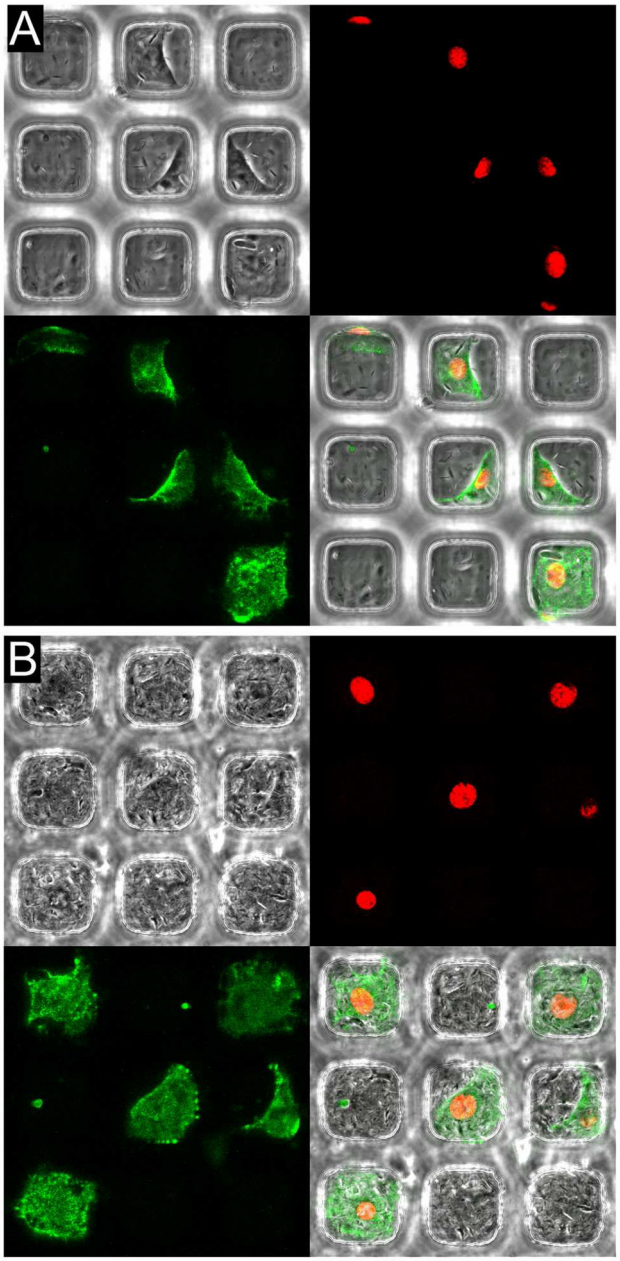

Figure 7. Immunofluorescent cellular imaging

NIH/3T3 cells expressing rat neu were plated onto micropallet arrays made from 1:50 and 1:10 FM1002F and stained with Hoechst 33342, a primary mouse antibody against neu and a fluorescently-labeled secondary anti-mouse antibody. Dual channel immunofluorescent imaging was performed using a scanning laser confocal microscope. Micropallets are 40 × 40 μm. (A, B) Micropallets are made from 1:50 FM1002F or 1:10 FM1002F, respectively. Disruption of signal in phase contrast images is increased with increased FeNP content, but the signals in fluorescent channels are largely unaffected.

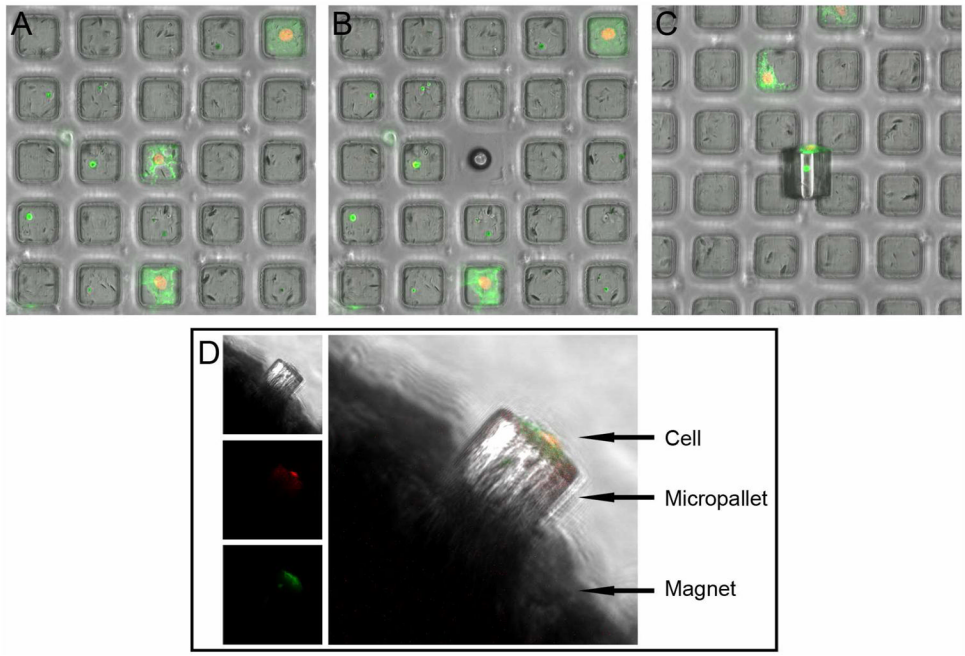

Figure 8. Release and collection of individual FM1002F micropallet and adherent cell

Single magnetic micropallets were released from the array using a laser and collected with a permanent magnet. (A) A micropallet holding a cell of interest is identified using microscopy. (B) The targeted micropallet is released by firing a pulsed laser focused at the glass-micropallet interface, which ablates micropallet material, producing rapidly expanding gas that ejects the micropallet from its position. Remnants of a bubble formed by the ablative process can be seen in the footprint from where the micropallet was released. (C) Released micropallet resting on the surface of the array, approximately 500 μm from its initial position. The cell remains adhered to the micropallet and minimally perturbed. At this point the magnetic collection probe is brought into proximity of the micropallet and the micropallet rises from its resting place and into contact with the probe. (D) The micropallet is magnetically attracted and held to the permanent magnet after collection. The cell remains adhered to the micropallet. The three left panels are the phase contrast (top) and the two fluorescent channels (nuclear stain; middle and rat neu surface marker; bottom) of the image separated for easier identification of the cell. It was noted that although the laser ablative technique of micropallet release delivers a concentrated dose of light energy, discernable photobleaching of the fluorescent markers has not been observed. The series of photomicrographs in this figure depict results that have been reproduced >50 x.

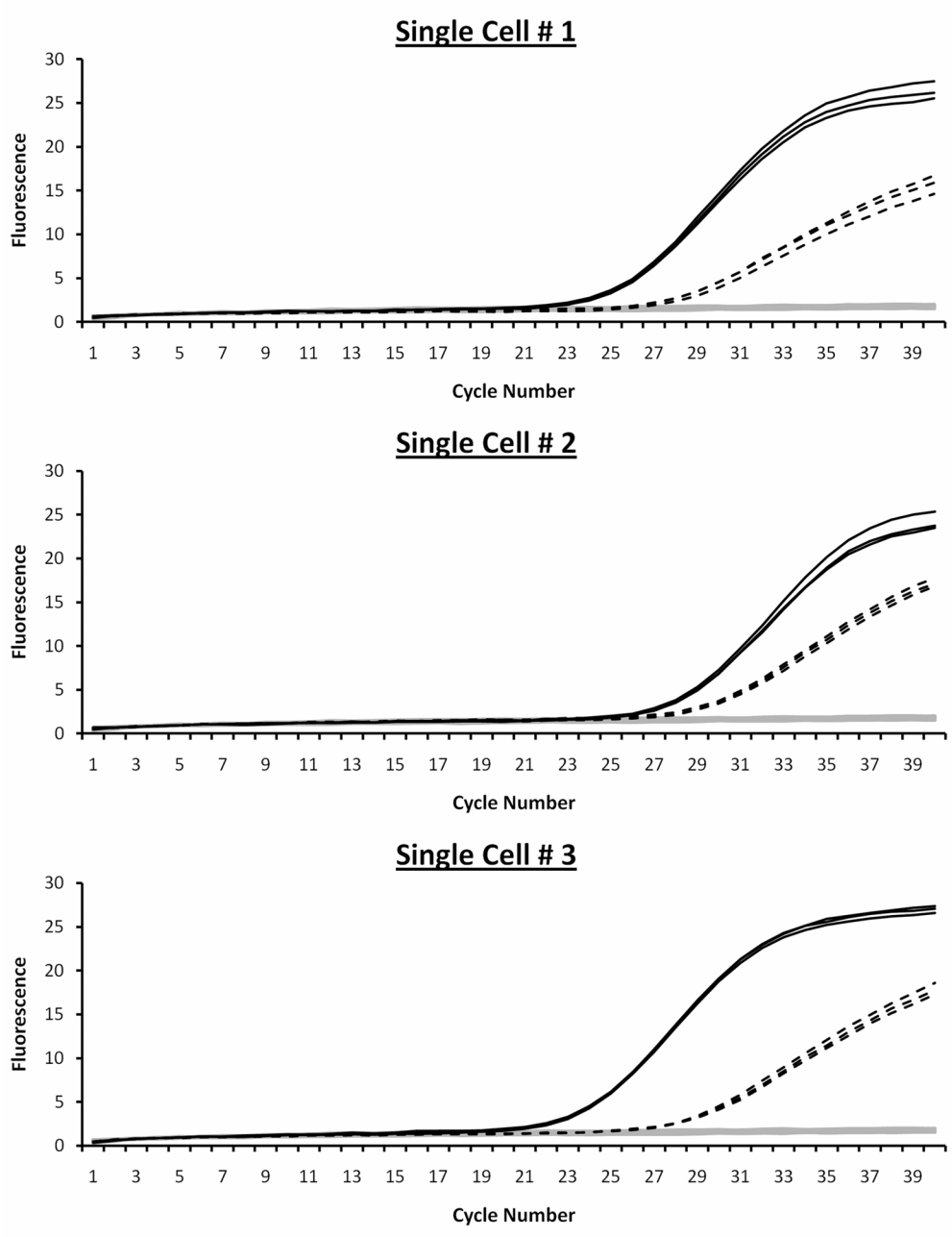

Figure 9. Single cell RT-qPCR

RT-qPCR traces from analysis of three separate cells collected on individual micropallets. Black solid lines show the amplification of rat neu (average for all three cells: Ct = 22.99 ± 2.2) and black dashed lines show the amplification of β-actin (average for all three cells: Ct = 26.80 ± 0.26), both of which were analyzed in triplicate for each single cell. NTC and –RT controls are both represented by gray lines. Rat neu and β-actin were detected for all single cell samples and all controls were negative for presence of cDNA.